Air Force Avionics Laboratory
Research and Technology Division
Air Force Systems Command
Wright-Patterson Air Force Base, Ohio

TRANSMITTER IMPEDANCE CHARACTERISTICS FOR AIRBORNE SPECTRUM SIGNATURE

Interim Technical Report No. 2
1 July - 30 September 1966

J. E. Ferris, W. DeHart, R. L. Wolford and W. B. Henry

15 October 1966

Contract AF-33(615)-3454

Contract Monitor: K. W. Tomlinson AVWE

7956-2-T = RL-2167

THE UNIVERSITY OF MICHIGAN
COLLEGE OF ENGINEERING
DEPARTMENT OF ELECTRICAL ENGINEERING
Radiation Laboratory

Administered through:
OFFICE OF RESEARCH ADMINISTRATION · ANN ARBOR

TABLE OF CONTENTS

ABSTRACT

An experimental technique for measuring the internal impedance of a source was developed under a previous contract, AF-33(615)-2606. The work described in this report is concerned with the evaluation of that technique. To facilitate the experimental evaluation, a device was needed to measure the relative power absorbed by a complex load. The design of such a device, an audio frequency subtractor, is presented.

To evaluate the linear model approach which serves as the basis for the impedance measurement technique, an investigation of the linearity of a real transmitter is being conducted. The transmitter linearity must be studied at harmonic and spurious frequencies as well as at the fundamental frequency. A measure of non-linearity can be drawn from a comparison of experimental and theoretical Rieke diagrams. Rieke diagrams at the second harmonic frequency for three power levels are presented and the results are discussed. The interaction between elementary generators of the multiple generator model representing the transmitter must also be given consideration. Thus, the variation of output power at the second harmonic frequency as a function of the load impedance at the third harmonic frequency has been measured. Conversely, the power variation at the third harmonic frequency as a function of the load at the second harmonic frequency has been obtained. The results are presented and discussed. Also included is a measurement of the transmitter's power amplifier plate efficiency.

I. INTRODUCTION

The statement of problem as set forth in the contract which provides for the present investigation is as follows:

(1) A determination of the power delivered to the antenna for "spectrum signature" purposes will require a measurement of the antenna impedance, transmission line characteristics, transmitter maximum power output, and transmitter output impedance at the fundamental, spurious and harmonic frequencies. The transmitter output impedance at the spurious and harmonic frequencies is not well understood and, therefore, requires further study. The prime payoff in this study will be better "spectrum signatures" for more accurate predictions of interference between systems.

(2) There is a requirement to verify the results of the earlier successful program, Contract AF 33(615)-2606 "Simplified Modeling Techniques for Avionic Antenna Pattern Signatures", with a mock-up of an aircraft transmitter system.

(3) The stated objective of the contract is: To conclude the development of "simplified" techniques for determining the RF spectrum signatures of flight vehicle electronics systems. To establish the validity of the techniques by comparing the results of data obtained by the "simplified" techniques with data obtained from tests employing a typical transmitter system in a mock-up.

(4) The present phase of the contract is concerned with the "simplified" technique that has been developed to allow a more accurate determination of the output impedance of a typical transmitter. The evaluation of this technique requires an investigation of the linearity of a typical transmitter at not only the fundamental frequency, but the harmonic and spurious frequencies as well.

II. SOURCE IMPEDANCE MEASUREMENTS

Techniques for measuring the output impedance of a source have been developed by the University of Michigan and were presented in the final report (Ferris, et al, 1966) on the predecessor contract. These techniques were derived from power transfer considerations of a linear mathematical model, i.e., the assumption is made that the source impedance is not a function of the load impedance. During the present contract an experimental investigation is being conducted to determine how closely a typical service transmitter conforms to this linear model. Appropriate adjustments of the model will be eventually required if the degree of non-linearity present in the transmitter is sufficient to make the linear model inaccurate.

2.1 Need for a Device to Measure the Relative Power Absorbed by a Complex Load

During the present investigation of power transfer in a coaxial system, there arose a need for a device calibrated to indicate relative power differences. The primary requirement of the device was the capability to measure the difference between two powers, P_i and P_r, after either power is arbitrarily varied. To meet this requirement, an audio-frequency subtractor was designed and constructed.

2.1.1 Design of an Audio-Frequency Subtractor

A block diagram of the subtractor is shown in Fig. 2-1.

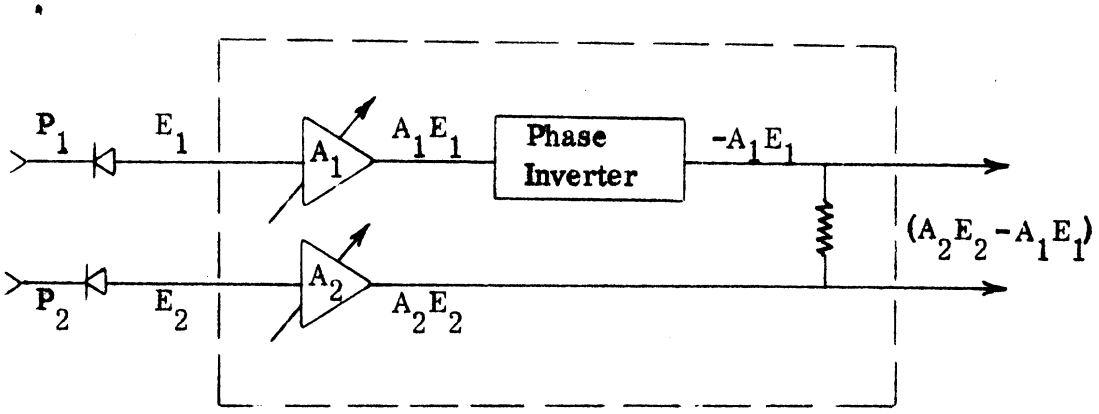

FIG. 2-1: A.C. Subtractor (Block Diagram)

Samples of two signals to be compared are detected by a square law detector. The outputs of the square law devices are voltages proportional to the power inputs;

$$E_1 = k_1 P_1, \qquad E_2 = k_2 P_2 \tag{2.1}$$

These voltages are amplified by a constant, the phase of one is shifted 180°, and they are added. The output is $(A_2E_2 - A_1E_1)$ where A is the amplifier gain. If $k_1A_1 = k_2A_2$ the output is proportional to the difference of the original power levels.

$$Ak\,(P_2 - P_1) = (A_2E_2 - A_1E_1) \tag{2.2}$$

One application of the subtractor is the measurement of the power consumed by a reactive load. A possible setup is given in Fig. 2-2. To calibrate the power measurement equipment, replace the variable load with a short circuit. With the short circuit in place, adjust the gain of the amplifier until the output is a minimum.

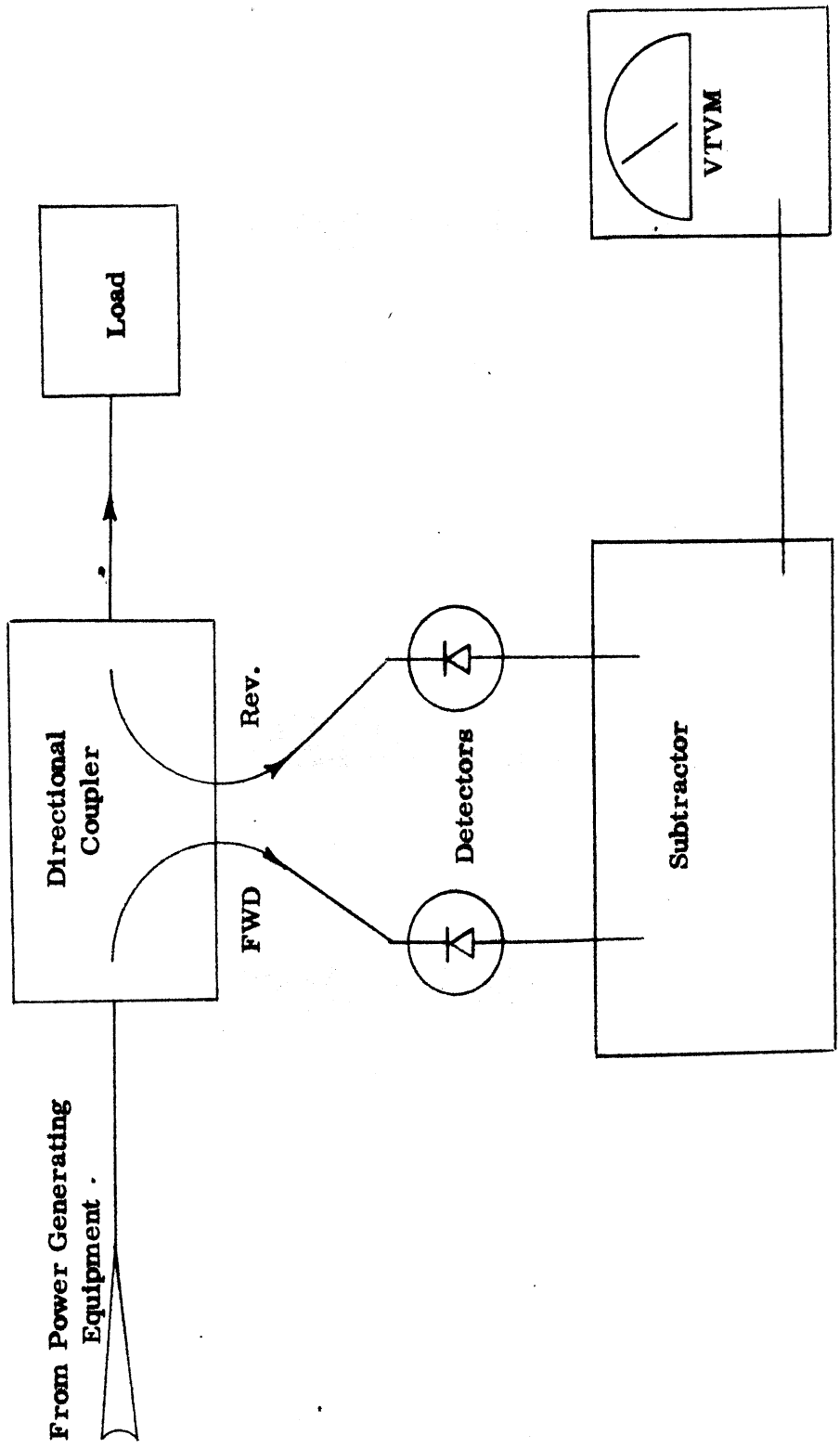

FIG. 2-2: POWER MEASUREMENT TEST SETUP

This will insure that all the constants within the system (different detector sensitivities, etc) have been normalized and that the output is proportional to the power differences. With the load connected, the relative power absorbed by the load can now be read directly from the meter scale. (The db scale on a H. P. 415 VSWR meter is especially convenient).

The device constructed is shown schematically in Fig. 2-3. The only adjustments are the feedback potentiometers used to control the gain of the amplifiers. The two amplifier stages are isolated except for the outputs. The input impedance of the amplifiers is about 20 kΩ and the output is approximately 50 kΩ. To insure linear operation, the input to the amplifiers must be limited to 0.1 volts peak to peak. The maximum output per stage is 5.0 volts peak to peak. For higher gain and lower noise operation, it is recommended that RCA 40233's or similar transistors be substituted for the 2N338A's presently installed. The design is flexible enough to allow a direct substitution of many silicon NPN transistors.

2.2 Source Non-Linearity at the Second Harmonic Frequency

In interim Technical Report 7956-1-T, source non-linearity was discussed and data was presented for the service transmitter RT-178/ARC-27 at the fundamental frequency (300 MHz). It was shown that non-linearity at the fundamental frequency is present, but is relatively small. Consideration must next be given to non-linearity at harmonic and spurious frequencies. Accordingly, an investigation of the second harmonic frequency was conducted by collecting data in the

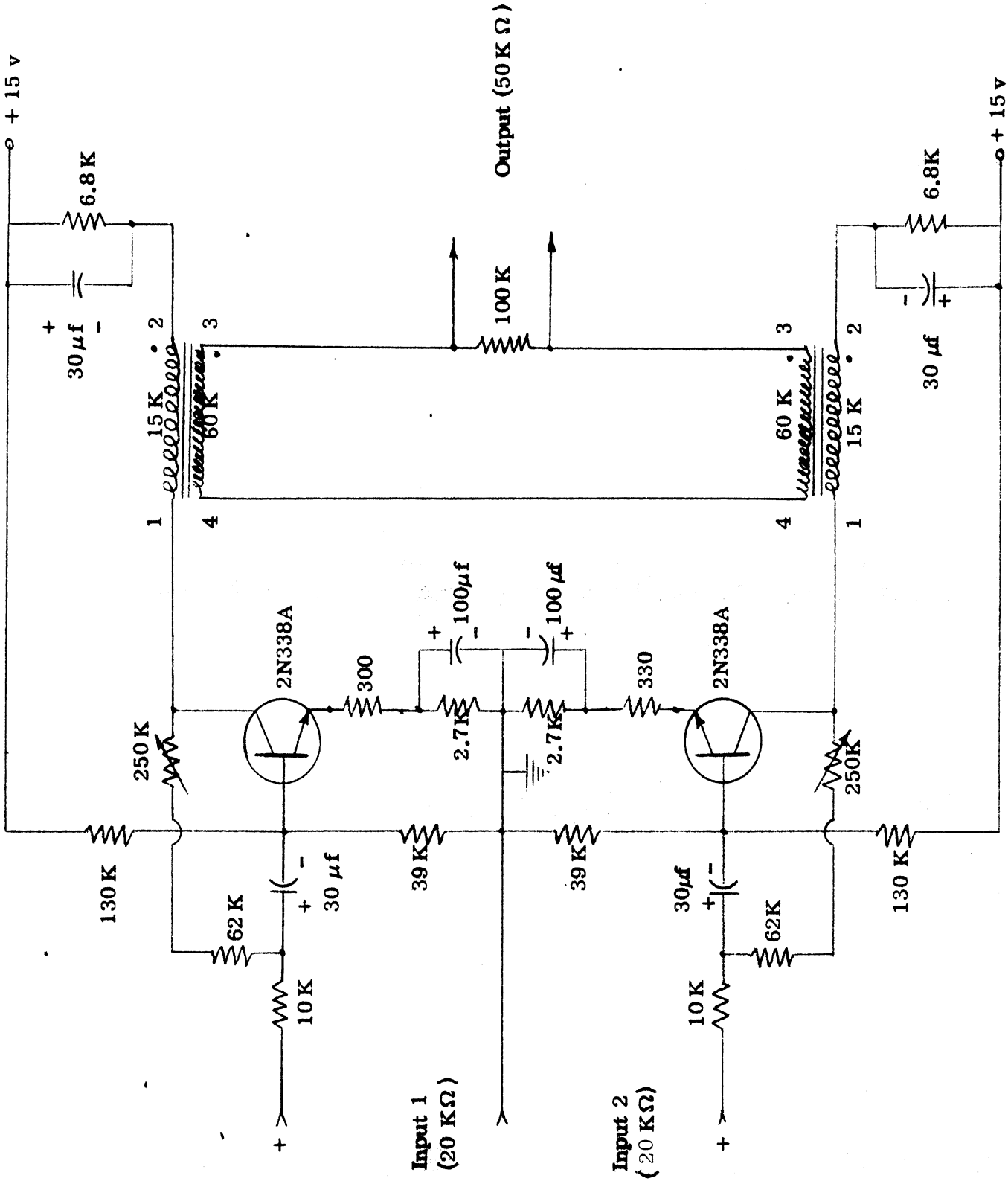

FIG. 2-3: A. C. SUBTRACTOR (Schematic)

form of Rieke diagrams. These diagrams are the most convenient tools by which to measure non-linearity. Experimental and theoretical Rieke diagrams are described in some detail in the above report.. Presented below are experimental and theoretical Rieke diagrams for the service transmitter and its linear model at the second harmonic frequency (600 MHz). The transmitter is seen at the right in Fig. 2-4.

2.2.1 Experimental Rieke Diagrams

To obtain experimental Rieke diagrams at 600 MHz, the equipment was arranged as shown in the block diagram of Fig. 2-5. The transmitter was operated in a large, well-shielded enclosure to prevent stray radiation from influencing the measurement equipment. The variable load presented to the transmitter consisted of a line stretcher, a variable attenuator, a shorted tuning stub, and a 50 Ω termination. The tuning stub was adjusted to provide a large reactance at the second harmonic frequency (600 MHz) while maintaining a matched termination at the fundamental frequency (300 MHz) and the third harmonic frequency (900 MHz). The line stretcher and attenuator were used to vary the phase angle and magnitude of the reactance, resulting in a load that was completely variable at 600 MHz. The power absorbed by the load at 600 MHz was monitored by means of a directional coupler and the audio-frequency subtractor discussed earlier in this report. The impedance of the second harmonic load was measured by means of the slotted line

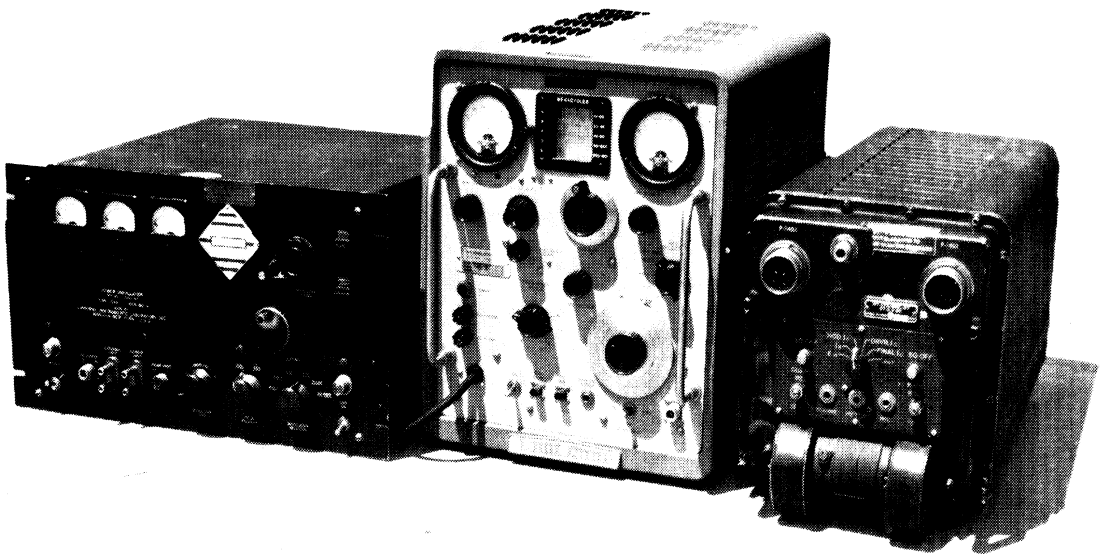

FIG. 2-4: AT RIGHT: SERVICE TRANSMITTER RT-178/ARC-27

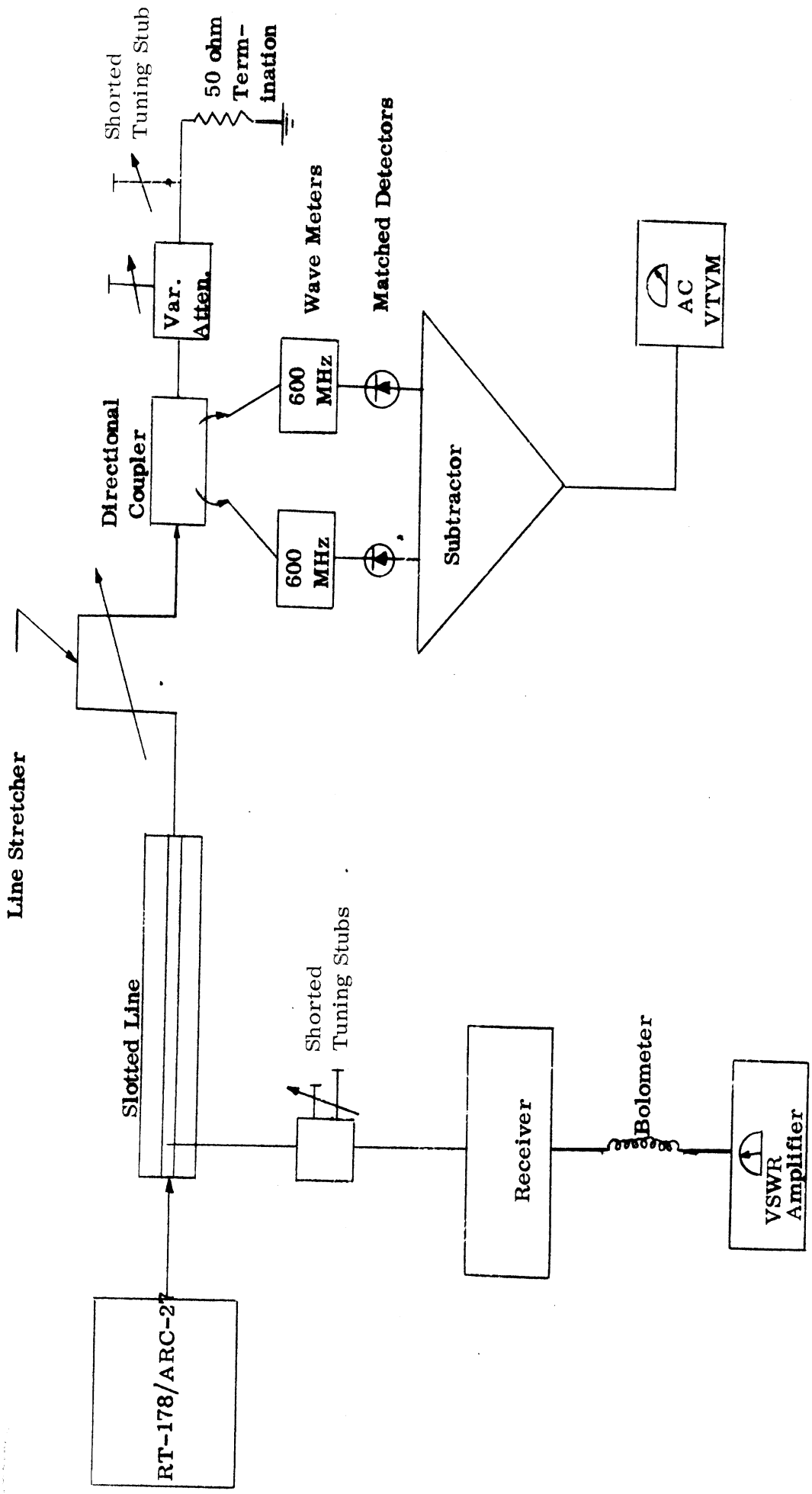

FIG. 2-5: Equipment Block Diagram for Experimental Rieke Diagrams at 600 MHz.

and frequency selective detection system consisting of a modified radar receiver, bolometer detector, and standing wave amplifier.

Figure 2-6 through 2-8 are three experimental Rieke diagrams obtained with the above equipment.

2.2.2 Theoretical Rieke Diagrams

Theoretical Rieke diagrams were calculated from a linear model like that shown in Fig. 2-9. The power contours for a constant source impedance will be circles on the Smith Chart with centers at $|\rho_o|$, β_o and with radii R_ρ, where

$$|\rho_o| = \frac{\left[\left(R_g^2 + X_g^2 - 1\right)^2 + 4X_g^2\right]^{1/2}}{\left(R_g - 1\right)^2 + K_n X_g^2}, \tag{2.3}$$

$$\beta_o = \tan^{-1}\left[\frac{-2X_g}{\left|R_g^2 + X_g^2 - 1\right|}\right] \tag{2.4}$$

$$R_\rho = \frac{\left[K_n^2 - 4K_n R_g\right]^{1/2}}{\left[R_g - 1\right]^2 + K_n + X_g^2}, \text{ and } K_n = 4R_g \frac{P_{max}}{P_n}. \tag{2.5}$$

The power contours for the linear model at the second harmonic frequency are shown in Figs. 2-6 through 2-8 superimposed on the experimental data points.

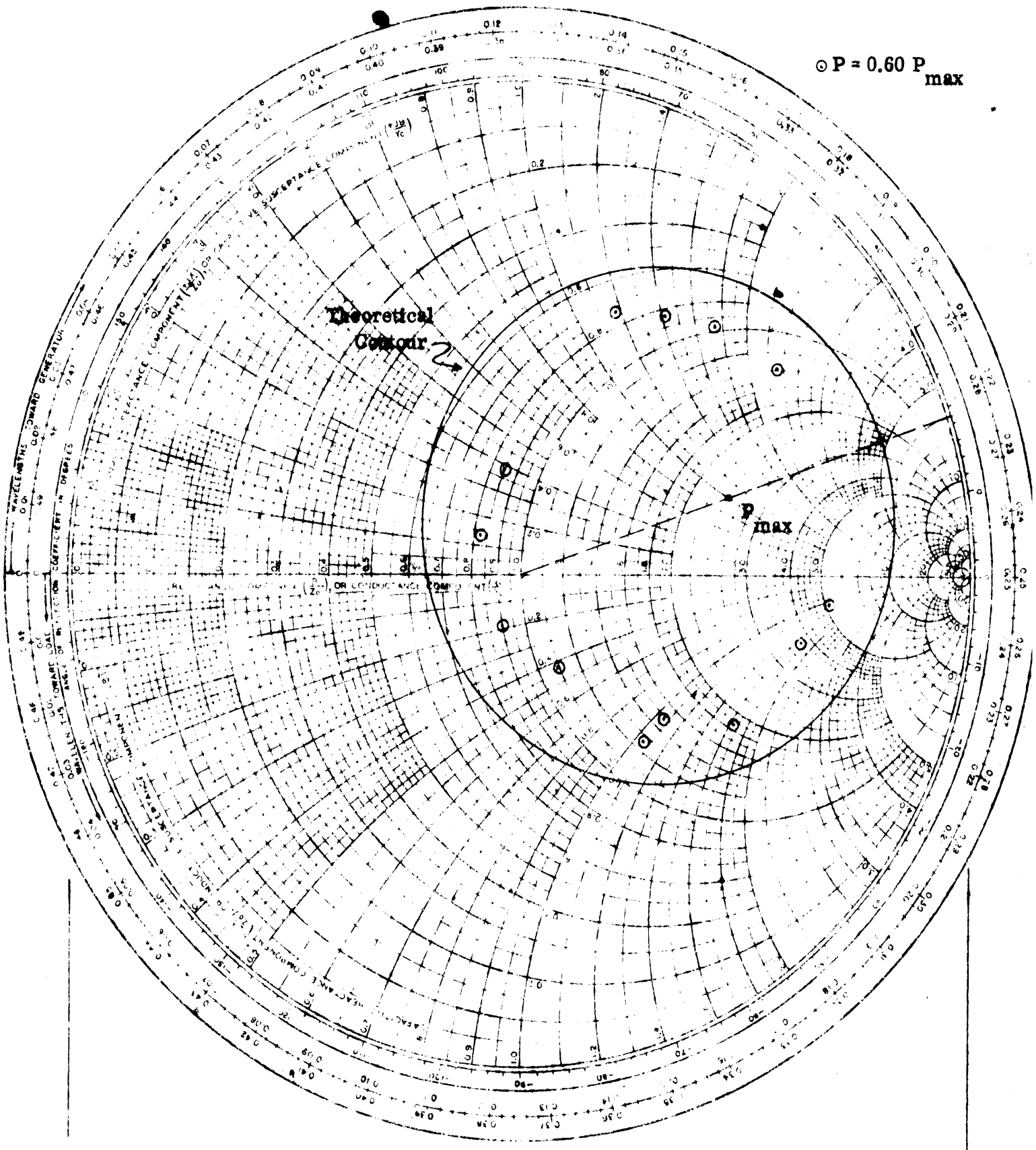

FIG. 2-6: Rieke Diagram of Transmitter RT-178/ARC-27 at the Second Harmonic Frequency (600 MHz)

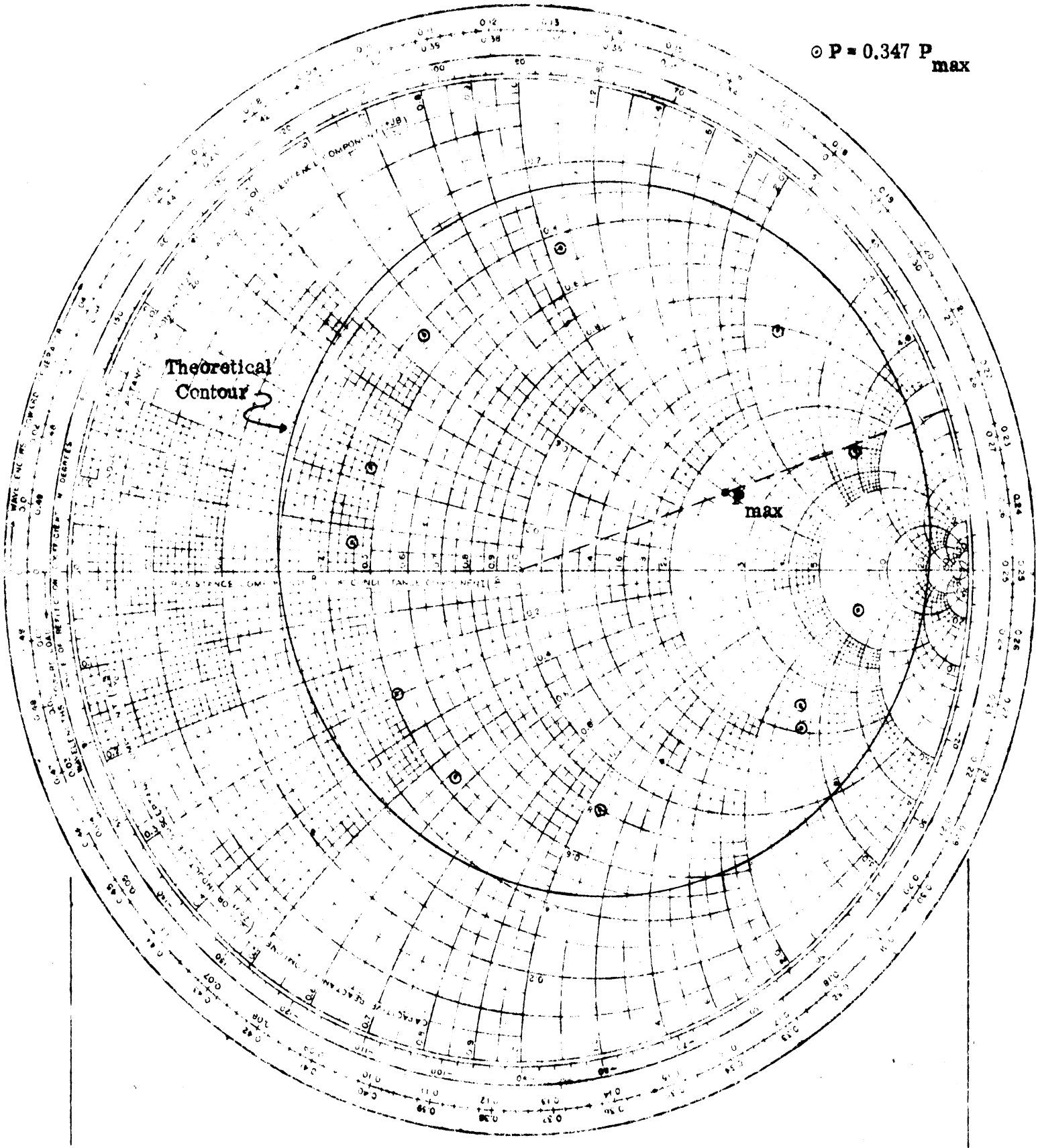

FIG. 2-7: Rieke Diagram of Transmitter RT-178/ARC-27 at the Second Harmonic Frequency (600 MHz)

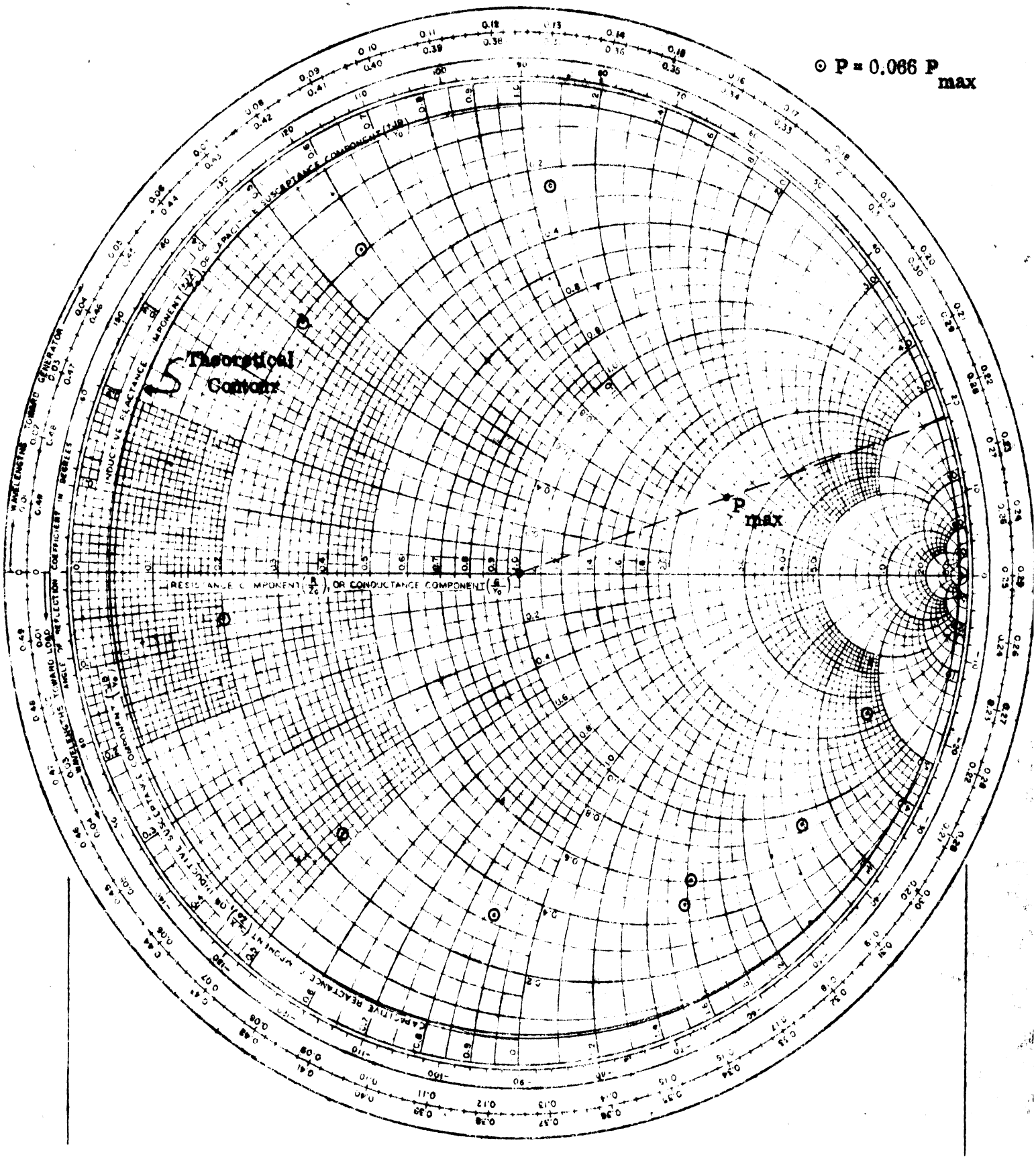

FIG. 2-8: Ricke Diagram of Transmitter RT-178/ARC-27 at the Second Harmonic Frequency (600 MHz)

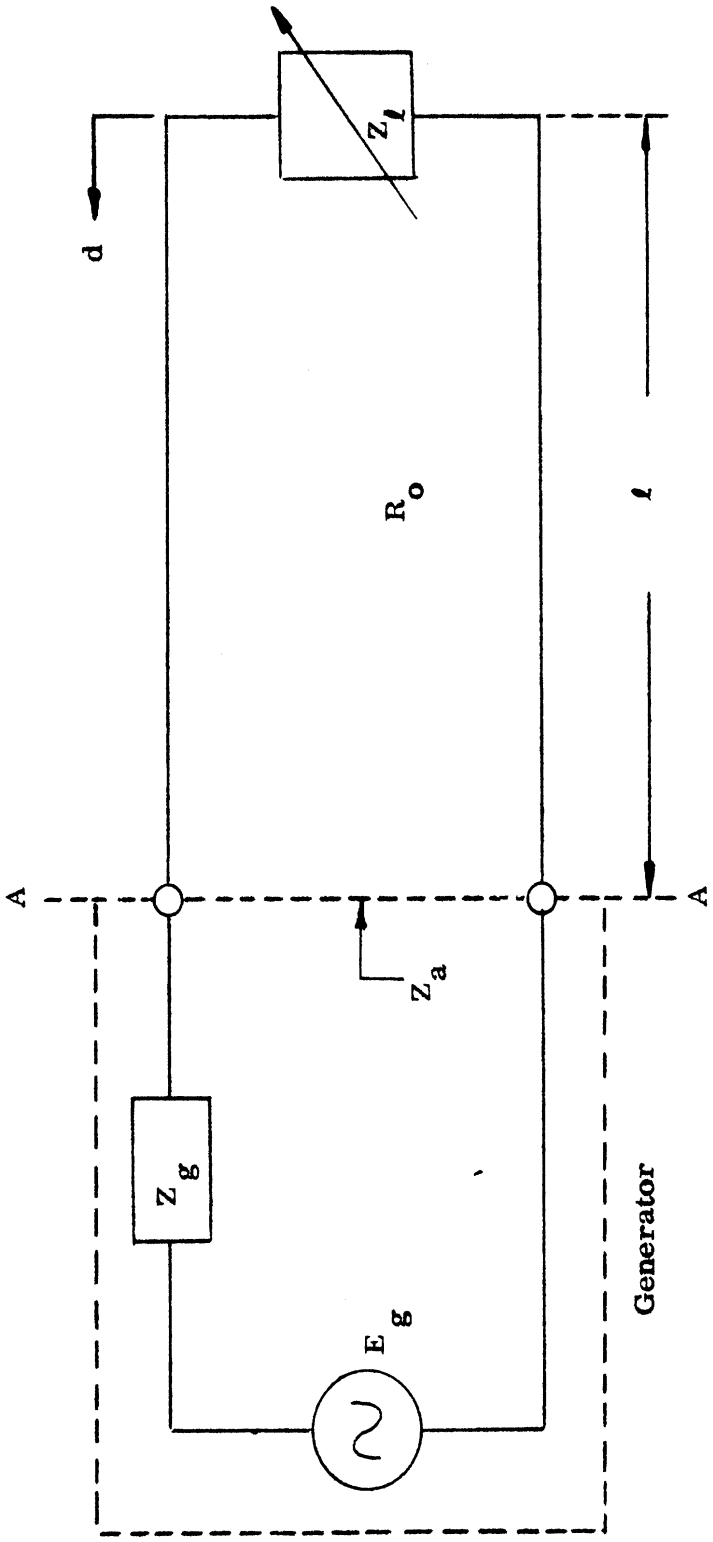

FIG. 2-9: SIMPLE POWER TRANSFER MODEL

2.2.3 Conclusions

A measure of the transmitter non-linearity at the second harmonic frequency is obtained by comparing the experimental power contours of the real transmitter with the theoretical power contours derived from the linear model. An inspection of the data in Figs. 2-6 through 2-8 indicates the presence of a small amount of non-linearity. The degree of non-linearity exhibited here is of the same order as that previously exhibited at the fundamental frequency and is felt that it is not sufficient to cause inaccuracy in the prediction of power transferred to the antenna at the second harmonic frequency. The difference in radii of the experimental and theoretical contours for each set of Rieke diagrams is not completely understood at this time and requires further study. It does not, however, reflect variation on the part of the transmitter's internal impedance.

III. SOURCE NON-LINEARITY DUE TO HARMONIC INTERACTION

In an investigation of source non-linearity at harmonic and spurious frequencies, consideration must be given to the aspect of source non-linearity at a given harmonic due to the interaction between the harmonics themselves. In the final report on the predecessor contract, a multiple generator model for spurious and harmonic frequencies was illustrated and the question of interactions between the elementary generators was discussed. If such a model is to be used to represent the transmitter outputs at each frequency present in the output spectrum, the linearity of each elementary model due to variations in the other elementary models must be investigated. No simple analytical treatment is known to the authors to prove or disprove this question. It is necessary to gather experimental evidence to determine the extent of interaction for a real transmitter.

3.1 Output Power Variations at the Second and Third Harmonic Frequencies

The military type RT-178/ARC-27 transmitter was connected into the measurement setup shown in Fig. 3-1, and the second harmonic (600 MHz) power delivered to a matched (50 Ω) load was measured as a function of the third harmonic (900 MHz) load. Inspection of the data in Fig. 3-2 reveals a total 600 MHz relative power variation of ± 1.7 db for 900 MHz load VSWR's ranging from 2.0:1 to 8.4:1. Measurements of the power at 900 MHz as a function of the load at 600 MHz were also performed utilizing the equipment arrangement of Fig. 3-3. The data is presented in Fig. 3-4.

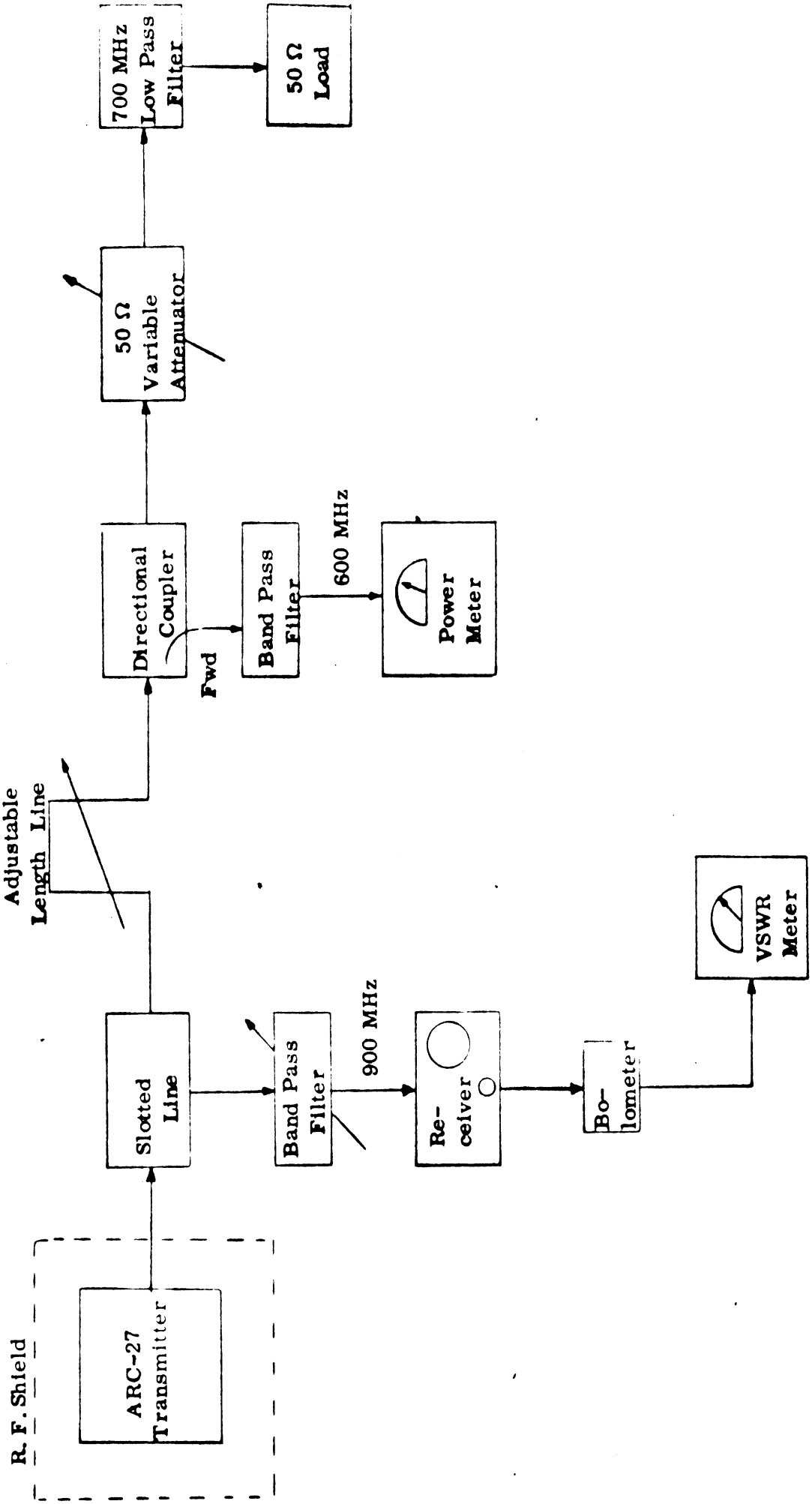

FIG. 3-1: 600 MHz HARMONIC INTERDEPENDENCE TEST BLOCK DIAGRAM

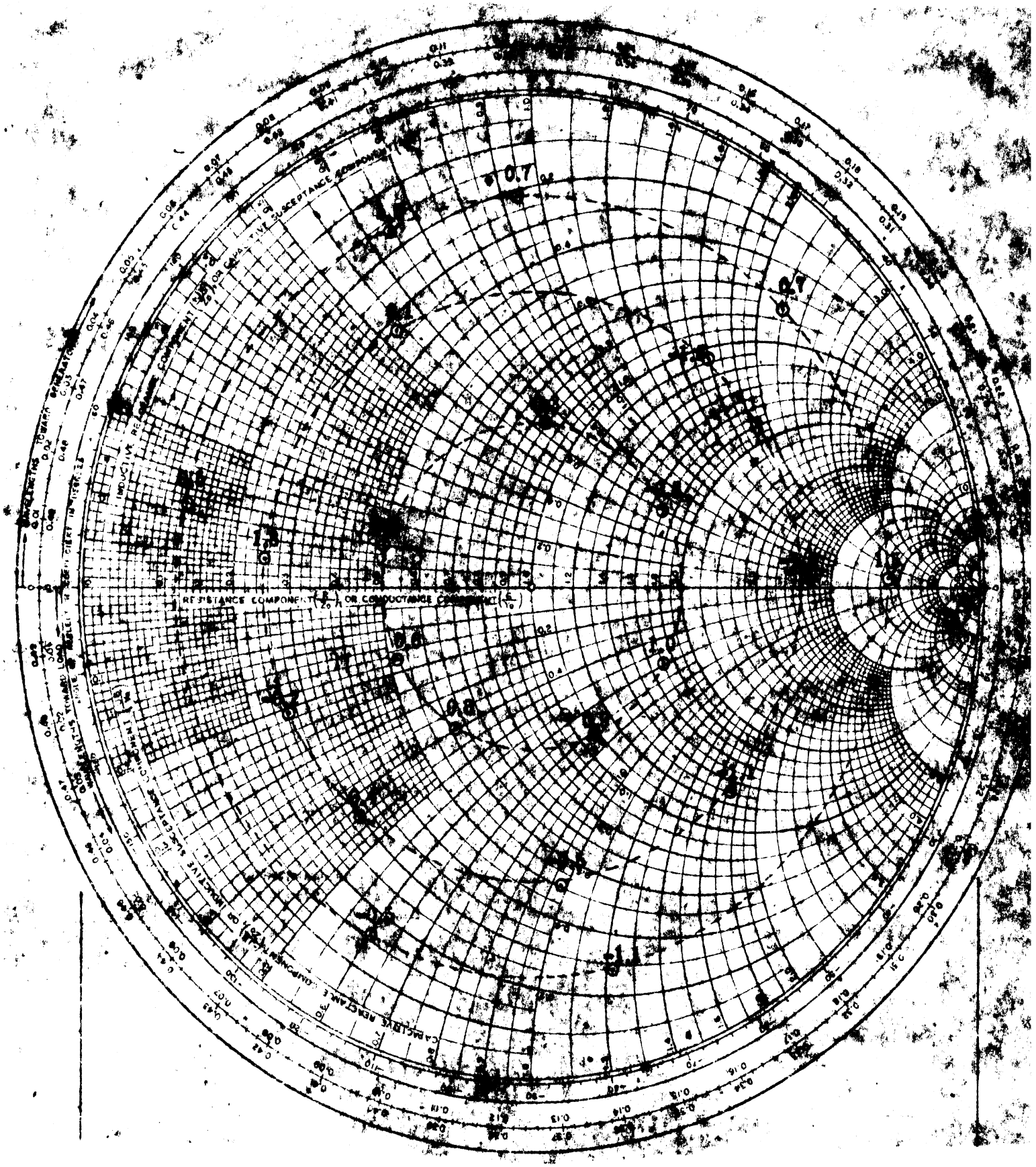

FIG. 3-2: RELATIVE POWER OUTPUT (db) AT THE SECOND HARMONIC FREQUENCY (600 MHz)

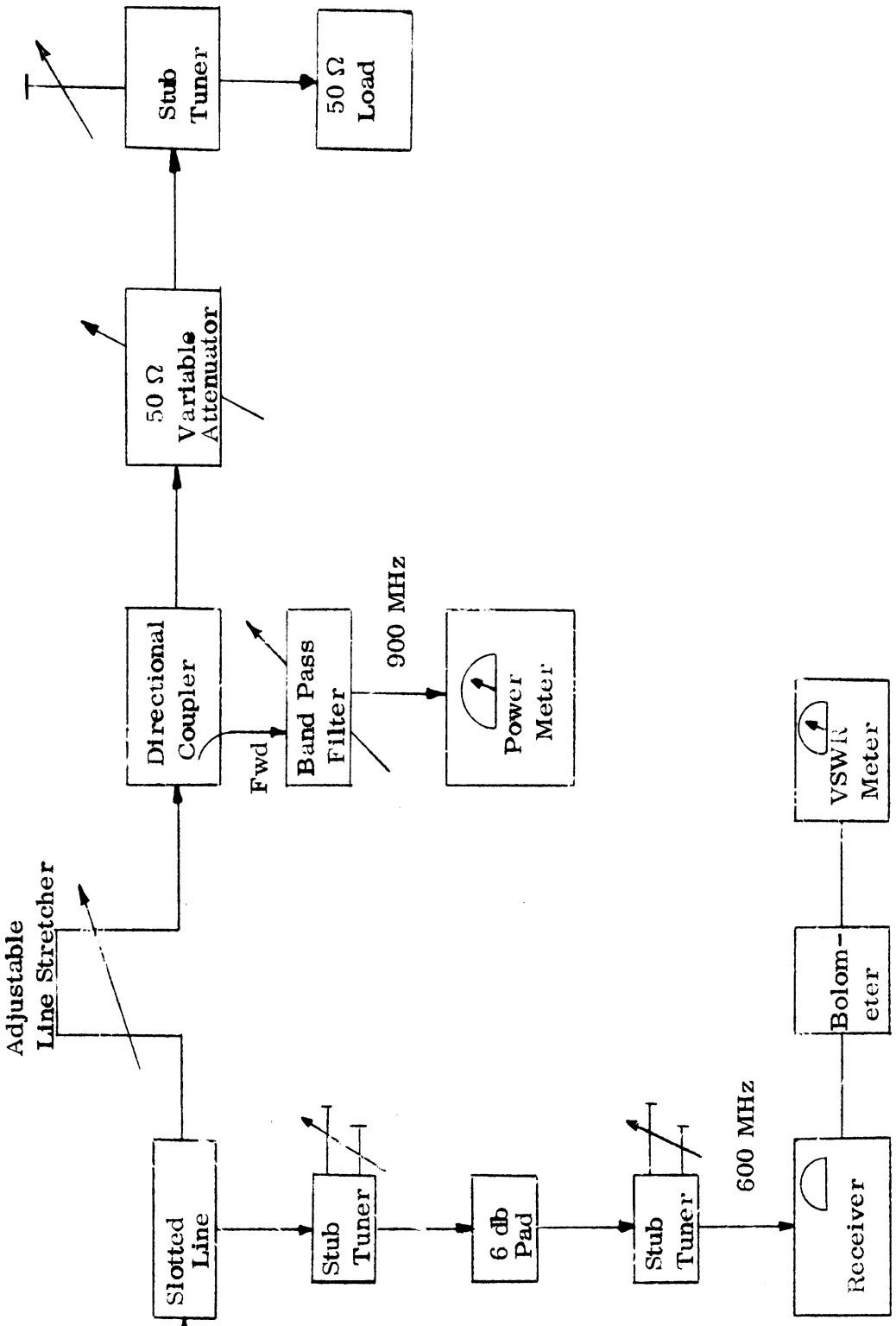

FIG. 3-3: 900 MHz HARMONIC INTERDEPENDENCE TEST BLOCK DIAGRAM

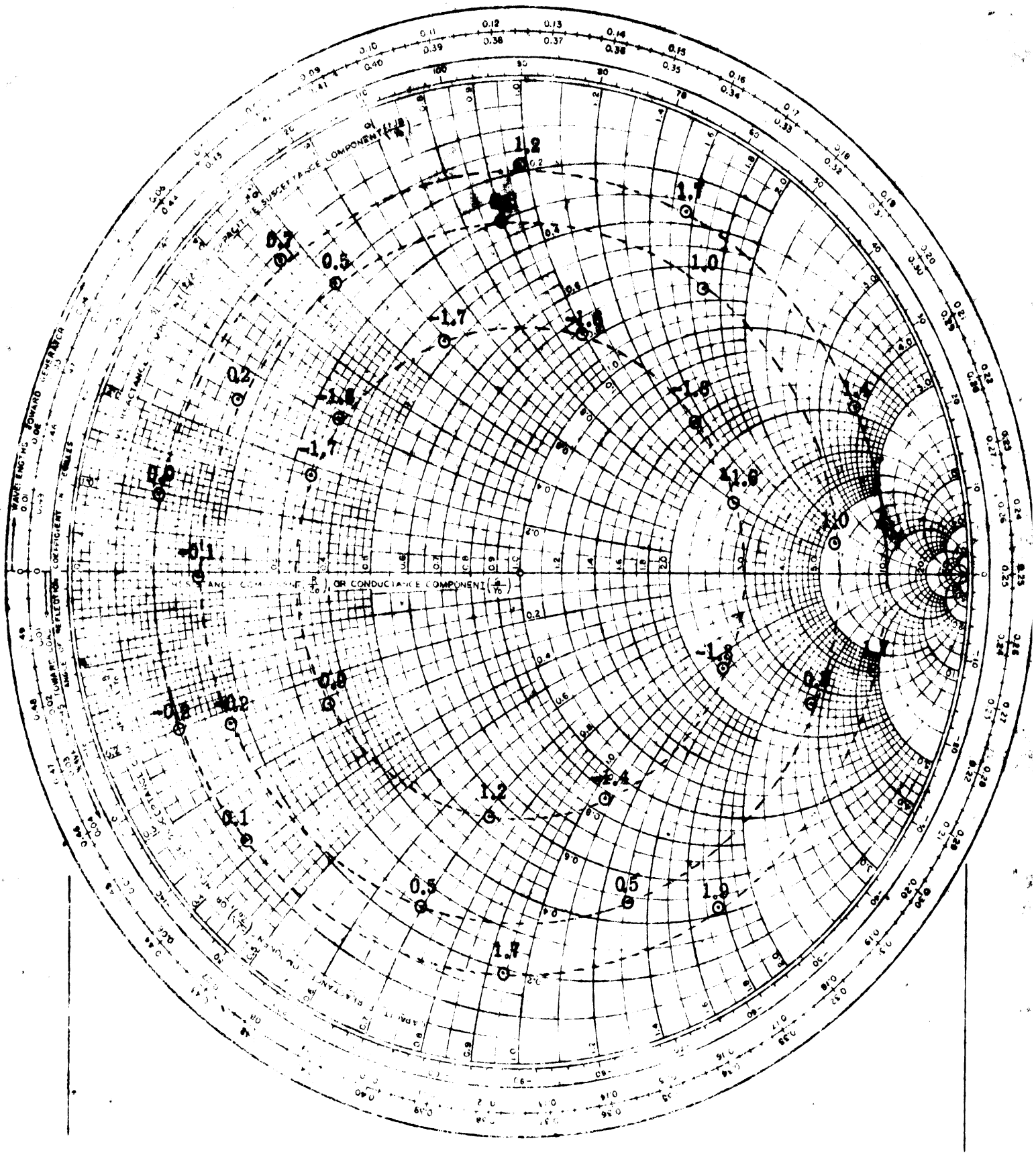

FIG. 3-4: RELATIVE POWER OUTPUT (db) AT THE THIRD HARMONIC FREQUENCY (900 MHz)

Note that there was a maximum power variation of ± 1.1 db at 900 MHz for a 10:1 VSWR at 600 MHz when the 900 MHz component was terminated in a matched load.

In view of the time and effort spent developing a suitable harmonic measurement technique, the measurement procedure will be discussed in some detail. One of the problems encountered was transmitter stray radiations. In spite of several cascaded frequency selective devices inserted between the slotted line probe and detector, measurements at the harmonics were being substantially influenced by a 300 MHz component. The source was traced to radiations from the transmitter which at the time was being operated without its external case to facilitate cooling. Installing the case solved the radiation problem, but imposed a relatively short transmitting duty cycle due to heating. Housing the transmitter and an auxiliary fan in a large, well-shielded cabinet proved adequate to contain the stray radiations and provide a long duty cycle. The transmitter output was investigated to determine if it was a function of the transmitter housing. There was no evidence that the output was influenced by the cabinet.

The impedance measurements were performed with a slotted line, receiver, bolometer detector, and a standard VSWR amplifier at both harmonics. The double stub tuners and fixed attenuator used to measure the 600 MHz load (Fig. 3-3) proved as selective as the band pass filter used at 900 MHz. The stub tuner arrangement also provided a gain in sensitivity since the attenuation of the band pass filter at the

pass frequency was nearly as great as the fixed pad used with the tuner, and in addition, the tuners allowed the probe to be matched to the receiver.

The loads and power measurement equipment were very similar for both measurements. Referring to Fig. 3-1, the 700 MHz low pass filter and a 50 Ω termination provided a matched load at 600 MHz and a high reactance at 900 MHz. The real part of the 900 MHz load impedance was varied with a 50 Ω variable attenuator, while a line stretcher provided continuously variable phase. In Fig. 3-3, a large reactance at 600 MHz was provided by a single shorted stub adjusted to $\lambda/2$ at 600 MHz. When so adjusted, the stub was $\lambda/4$ at 300 MHz and $3/4\lambda$ at 900 MHz, allowing these frequencies to be terminated by the matched 50 Ω load. The impedance at 600 MHz was varied with a line stretcher and variable attenuator as described above.

The power measurement equipment consisted simply of a directional coupler, band pass wavemeter, and power meter. The power sampled at the incident port was proportional to the power absorbed by the load since the load was matched at the frequency of interest.

3.2 Conclusions

The non-linearity due to interactions of the second and third harmonic frequencies for the RT-178/ARC-27 service transmitter does not appear to be severe when the frequency component being investigated is terminated in a 50 Ω load. The

inter-harmonic effects represented by the data in Figs. 3-2 and 3-4 can be explained at least qualitatively in terms of non-linear mixing. Suppose that the power transferred to a load in a coaxial system consists of the fundamental component, P_1 plus components at harmonically related frequencies P_2, P_3, $P_4 \ldots P_n$. If the load is perfectly matched to the source at all frequencies present, all of the power will be absorbed by the load. Suppose now that the load is not perfectly matched. Some portion of each original component will be reflected back to the source. If the source is a vacuum-tube amplifier (or any device characterized by a non-linear voltage-current relationship), the reflected components will combine with the original components producing a new spectrum consisting of components at every possible sum, difference, and harmonically related frequency. The magnitudes of the new spectrum components will be a function of the circuit parameters and the magnitude and phase of each mixing component. It is evident at this point why the sheer magnitude of the number of frequencies coupled with a less than thorough knowledge of vacuum-tube non-linearities has thus far hindered a precise mathematical approach to this problem.

In the particular instance investigated, the signal source was the ARC-27 transmitter. The power output at the second harmonic frequency was investigated as a function of the load impedance at the third harmonic frequency and vice-versa. Notice that the frequency difference of the two harmonics is simply the fundamental

frequency. The magnitude of the second harmonic power must include a term which is a function of the magnitudes and phases of the fundamental and third harmonic frequencies. In other words, the variation of the second harmonic power as a function of the load at the third harmonic was due to a variation of the magnitude and phase of the reflected third harmonic component, which in turn mixed with the fundamental component causing a changing resultant at the second harmonic. The changes in the third harmonic power as a result of a varying load at the second harmonic follows from a similar argument.

The measurement of harmonic interaction should be extended to the case in which the frequency in question is not terminated in a 50 Ω load. For measurements similar to those in Fig. 3-2, the load should consist of a 50 Ω termination at 300 MHz, a fixed mismatch at 600 MHz (the frequency in question) and a continuously variable impedance at 900 MHz. Such a load is presently under consideration.

IV. SOURCE EFFICIENCY

A measurement of the plate efficiency of the RT-178/ARC-27 transmitter has been obtained. This measurement was performed to enable the transmitter to be classified with others on the basis of the operating condition of its power amplifier stage. An efficiency of 58 per cent has been calculated from measurements of RF output power and DC power supplied in the plate circuit. However, due to the fact that the power amplifier employs the grounded-grid system, the figure of 58 per cent cannot be attributed solely to the power amplifier stage, but is a combination of this stage and the preceeding (driver) stage. A reasonable figure for the power amplifer stage alone would be between 25 and 50 per cent. The grounded-grid system is probably employed to negate the need for a neutralizing system, and thereby increase the efficiency obtainable from a particular vacuum-tube for a given bandwidth.

REFERENCES

Ferris, J.E., et al (1966), "Investigation of Measurement Techniques for Obtaining Airborne Antenna Spectrum Signatures," Final Report AFAL-TR-66-101, July, 1966, University of Michigan Radiation Laboratory Report 07274-1-F, 137 pages.

Ferris, J.E., et al (1966), "Transmitter Impedance Characteristics For Airborne Spectrum Signature", Interim Technical Report No. 1, July, 1966, University of Michigan Radiation Laboratory Report 7956-1-T, 35 pages.